

Long-Range Correlations in Sedimentation

P. N. Segrè,* E. Herbolzheimer, and P. M. Chaikin†

Corporate Research Science Labs, Exxon Research and Engineering Company, Route 22 East, Annandale, New Jersey 08801
(Received 23 May 1997)

Using particle image velocimetry we have measured the sedimentation dynamics of non-Brownian colloidal spheres over a wide range of low concentrations ($\phi \leq 0.05$) and sample cell sizes W . Fluctuations in the settling velocity show universal large-scale finite-range correlations, in the form of swirls, which depend simply on volume fraction and particle radius and follow $\langle \delta V_z(0) \delta V_z(z) \rangle^{1/2} \approx 2.0 V_{\text{sed}} \phi^{1/3} \exp(-z/2\xi)$, where $\xi \approx 20a\phi^{-1/3}$. In turn, the predicted divergence of the velocity variance with increasing cell size W is cut off in a universal way as W exceeds the swirl size and is well represented by $\langle \delta V_z^2(0) \rangle^{1/2} = 2.0 V_{\text{sed}} \phi^{1/3} [1 - \exp(-W/60a\phi^{-1/3})]$. [S0031-9007(97)04086-6]

PACS numbers: 82.70.Dd, 05.40.+j, 66.20.+d, 66.90.+r

Understanding of the sedimentation properties of monodisperse spherical particles in a quiescent liquid is still far from complete. For particles that are large enough to neglect Brownian motion, dilute enough so that we can ignore the direct interparticle interactions, and in a highly viscous fluid so that inertia is irrelevant, the settling dynamics and the density and velocity correlations are determined completely by the long-range ($\sim 1/r$) hydrodynamic interactions. Differences in individual particle velocities about the mean settling rate, the subject of this Letter, arise from local density fluctuations that occur during sedimentation.

In recent years several apparently conflicting theories and experiments describing the amplitudes of the velocity fluctuations have been reported. On the one hand, simple theoretical arguments [1] as well as computer simulations with up to 32 768 particles [2] have indicated that the magnitudes of such fluctuations might diverge with increasing cell size. On the other hand, larger scale experiments [3,4], and a more detailed theory [5], have found no evidence for such divergences. The fluctuation magnitudes have generally been found to be of the order of the settling velocity [4,6,7], although much smaller values have been reported in the most dilute samples [8,9].

In this Letter we describe several experimental findings. First, in samples that range in concentration over nearly 3 orders of magnitude, we found that the velocity fluctuations exhibit characteristic correlated regions, or swirls, of size $\xi \approx 20$ mean interparticle spacings. Second, over the same concentration range, the fluctuation amplitudes scale as $V_{\text{sed}} \phi^{1/3}$. A simple model is developed which shows that these two results are consistent with each other. Finally, the velocity fluctuation amplitudes display a cell size dependence only for cells whose dimensions are less than the characteristic swirl size, and no evidence for diverging fluctuations are found. The results of these and all previous experiments can be collapsed onto a universal curve which depends on the ratio of the cell size to the swirl size.

The colloidal particles used in our experiments were monodisperse polystyrene spheres of radius $a = 7.8 \pm$

$0.1 \mu\text{m}$ purchased from Bangs Lab Inc. They were dispersed in water with a small amount (0.01% by weight) of sodium dodecyl sulfate surfactant added to prevent aggregation. Particle interactions can be considered to be near those of hard spheres. The sample cells consisted of several sealed rectangular glass tubes varying in width \times depth \times height from $3 \times 0.3 \times 50 \text{ mm}$ to $30 \times 10 \times 200 \text{ mm}$, as well as a 0.5 mm radius cylinder of height 30 mm . The cells were placed in a large stirred water bath controlled at $T = 23 \pm 0.1 \text{ }^\circ\text{C}$.

A single isolated sphere in our experiments settles at the well known Stokes velocity $V_0 = \frac{2}{9} a^2 \Delta \rho g / \eta \approx 6.5 \mu\text{m}/\text{sec}$, where $\Delta \rho$, g , and η are, respectively, the density difference between polystyrene and water, the gravitational constant, and the viscosity of water. The Peclet number is $\text{Pe} = V_0 a / 6D > 10^4$, with D being the Brownian diffusion coefficient. Thus, the settling motions dominate those due to Brownian diffusion. The particle Reynolds number $\text{Re} = 2aV_0\rho/\eta \approx 1.2 \times 10^{-4}$, so inertial effects are negligible. To discern the specific role of the hydrodynamic interactions, we only observed samples in the dilute limit, $0.01\% \leq \phi \leq 5\%$.

Particle velocities were measured using the technique of particle image velocimetry (PIV) [10]. The apparatus consists of a (1024×1320 pixels) charge-coupled device camera, a light source placed behind the cell, and some specialized image processing software and hardware purchased from Dantec Instruments. The camera was focused in the median plane of the cell, and the depth of field was approximately $1/2 \text{ mm}$. A large cross section of the cell was imaged (typically $4 \times 5 \text{ mm}$), so that several thousand particles could be simultaneously studied. Each particle spanned across several dozen pixels. Initially, random dispersions were prepared by vigorous shaking of the cells, and measurements began after the visible sedimenting front had settled a sizable fraction, about $1/5$, of the cell height. The location of the imaging window was far from both the sedimentation front and the sediment growth. In a typical experiment, two images were acquired, separated in time by approximately the time it takes an average particle to settle its own diameter, $\sim 3 \text{ sec}$. The 2D

velocity fields consisting of a “map” of $\sim 30 \times 40$ vectors was then extracted by comparing the two pictures using standard PIV techniques and determining the local particle displacements that had occurred between them. In practice, each velocity vector was the local average of the displacements of two to four spheres. Velocity fluctuations were then found by numerical subtraction of the mean settling velocity from the measured velocity field. Calibration tests performed on translating grid patterns drawn on paper aided in the optimization of the system parameters and demonstrated accuracies of order 1%–2%.

Figure 1 displays typical PIV results taken at two representative volume fractions, $\phi = 0.01\%$ and 3.0% . Figures 1(a) and 1(d) show the measured vector maps of the settling spheres which clearly demonstrate that the variance in local velocities is considerably larger in the more concentrated sample. To examine the fluctuations explicitly we display in Figs. 1(b) and 1(e) the velocity vectors determined by subtracting the measured mean sedimentation rates, i.e., $\delta \mathbf{V}_i = \mathbf{V}_i - \mathbf{V}_{\text{sed}}$, where $\mathbf{V}_{\text{sed}} = \langle \mathbf{V}_i \rangle$. As a result, the fluctuations in the sample of lower concentration become more apparent. Regions of correlated velocities, or swirls, are seen in the corresponding fluctuation flowlines shown in Figs. 1(c) and 1(f). The swirls are bigger in the more dilute sample than in the concentrated one. (As we shall see they scale with respective mean interparticle distances $n^{-1/3} = (4\pi/3)^{1/3} a \phi^{-1/3}$ for a space fill-

ing simple cubic lattice, with n being the number density.) In both cases the swirl sizes are larger than the particle diameters, $2a = 0.015$ mm, and considerably smaller than the cell size, $W = 20, 10$ mm for $\phi = 0.01\%$, and 3% . Each swirl contains ~ 3000 particles.

We begin our analysis with the spatial correlations in the velocity fluctuations. The normalized autocorrelation function of the z component (\parallel to the sedimentation) of the velocity fluctuations can be defined as

$$C_z(\mathbf{r}) \equiv \langle \delta V_z(0) \delta V_z(\mathbf{r}) \rangle / \langle \delta V_z(0)^2 \rangle, \quad (1)$$

where $\langle \dots \rangle$ represents an ensemble average from several hundred individual runs taken over long periods of time and using several different preparations. We shall take the distance vector \mathbf{r} either in the direction parallel to the sedimentation, $C_z(z)$, or perpendicular to it, $C_z(x)$.

The inset of Fig. 2(a) displays $C_z(z)$ for four representative volume fractions. These correlation functions exhibit a roughly exponential decay, as $C_z(z) \sim \exp(-z/\xi_{\parallel}^z)$. On the other hand, the correlations in the horizontal direction, $C_z(x)$ [Fig. 2(b) inset] show rapid initial decays followed by distinct regions of (small) negative amplitude, the minima of which are defined to be at ξ_{\perp}^z . In combination, these lead to a qualitative picture for the average flow pattern as consisting of vertically elongated rotating swirls or short columns of particles with

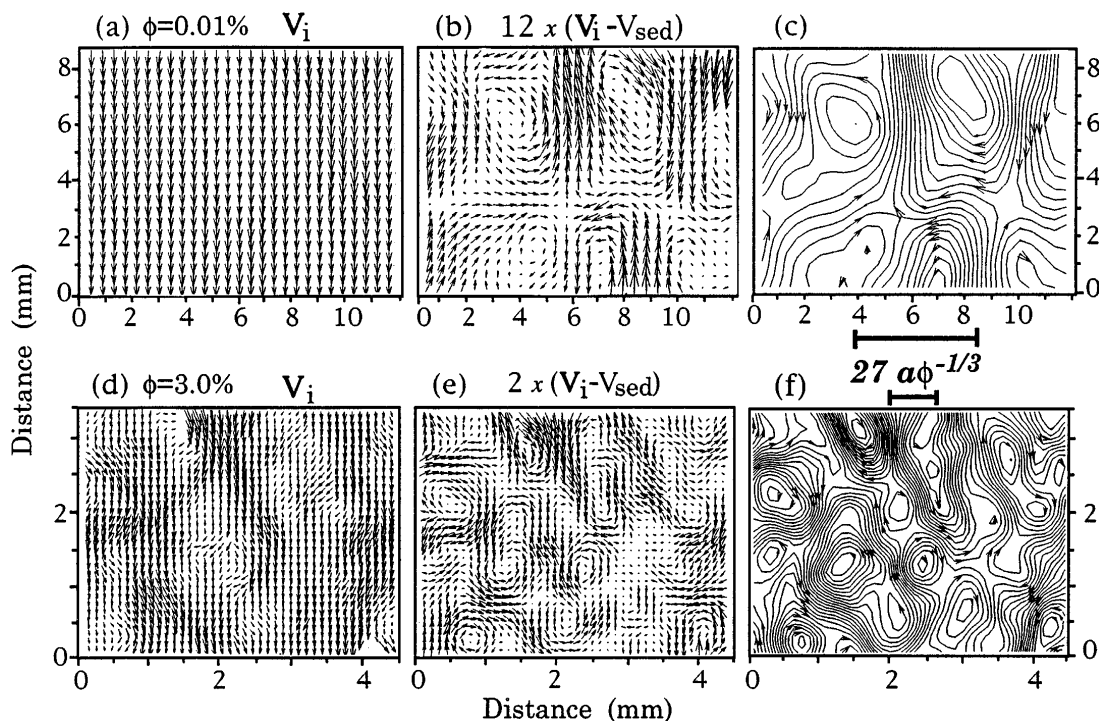


FIG. 1. PIV results for two suspensions of sedimenting polystyrene spheres at $\phi = 0.00010$ (a)–(c) and $\phi = 0.030$ (d)–(f). (a),(d) Measured velocity vector maps. Each vector V_i represents the velocity of a region of two to four particles. (b),(e) Velocity fluctuations calculated from (a),(d) as $\delta \mathbf{V}_i = \mathbf{V}_i - \langle \mathbf{V}_i \rangle$. Note the different magnifications of the vector scales used for clarity. (c),(f) Velocity fluctuation flow lines. The distance bars drawn are the characteristic correlation lengths, $\xi_{\perp}^z = 27a\phi^{-1/3}$, found in Fig. 2(b).

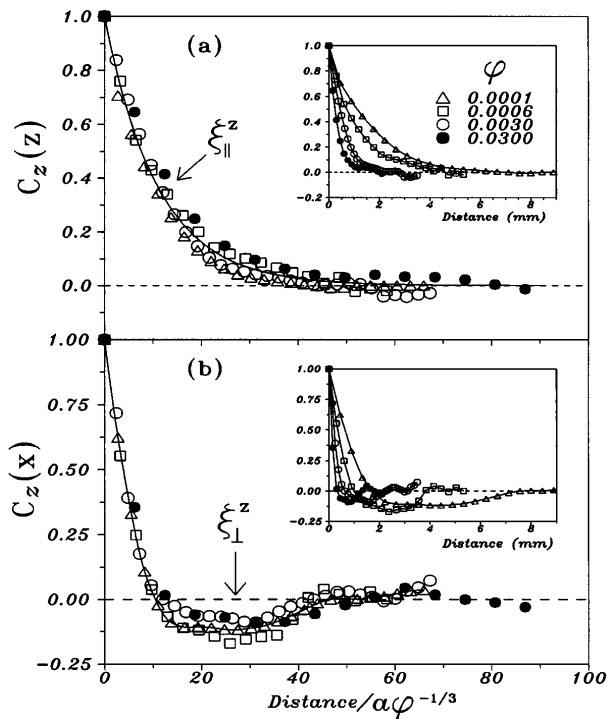


FIG. 2. Spatial correlation functions of the z component of the velocity fluctuations as a function of distance (a) parallel and (b) perpendicular to the z axis for four representative volume fractions. In the insets the data are plotted versus distance, while in the main figures distance is scaled by $a\phi^{-1/3}$. The lines drawn are (a) $C_z(z) = \exp(-z/11a\phi^{-1/3})$, and (b) a guide to the eye.

characteristic dimensions of $\xi_{\perp}^z \times 2\xi_{\parallel}^z$. Evidence for this picture can also be seen in the flow lines of Fig. 1.

The main Figs. 2(a) and 2(b) display the velocity correlations plotted versus distance scaled by $a\phi^{-1/3}$. Remarkably, over the 300 fold increase in volume fraction we studied, a near collapse of both $C_z(z)$ and $C_z(x)$ is seen. The dependence of the correlation length can be written as

$$\xi_{\parallel}^z \approx 11a\phi^{-1/3}, \quad \xi_{\perp}^z \approx 27a\phi^{-1/3}. \quad (2)$$

The amplitudes of the velocity fluctuations in the directions parallel and perpendicular to the flow direction are defined as $\Delta V_{\parallel} \equiv \sqrt{\langle [V_z - V_{\text{sed}}]^2 \rangle}$ and $\Delta V_{\perp} \equiv \sqrt{\langle V_x^2 \rangle}$. As seen in Fig. 3, the fluctuations are found to increase as $\phi^{1/3}$. The magnitude of the parallel fluctuations are always larger than those in the perpendicular direction. Overall, the data can be well fitted by

$$\frac{\Delta V_{\parallel}}{V_{\text{sed}}} = (2.0 \pm 0.1)\phi^{1/3}, \quad \frac{\Delta V_{\perp}}{V_{\text{sed}}} = (1.0 \pm 0.05)\phi^{1/3}. \quad (3)$$

It is interesting to note that the data of Nicolai *et al.* [6], obtained using an imaging technique at higher concentrations, $0.05 \leq \phi \leq 0.2$, agree fairly well with the extensions of our low- ϕ power law fits.

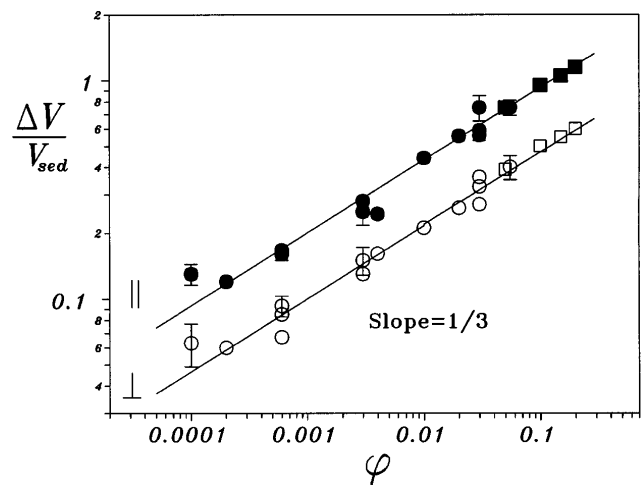


FIG. 3. Normalized velocity fluctuation amplitudes $\Delta V/V_{\text{sed}}$, \parallel (closed symbols), and \perp (open symbols), to the sedimentation direction, versus volume fraction ϕ . Circles, this work; squares are from Ref. [6]. Data are from large cells of widths $W \geq 150a\phi^{-1/3}$. ($W \sim 100a\phi^{-1/3}$ from Ref. [6]).

We now turn to the description of the effects of the cell size on the velocity fluctuations during sedimentation. To review, the results for all ϕ in Figs. 1–3 were obtained from *large* cells of widths $W > 150a\phi^{-1/3}$, and characteristic swirls of width $\xi_{\perp}^z \approx 27a\phi^{-1/3}$ were found. Nonzero correlations extended out roughly only twice ξ_{\perp}^z , still less than the relevant cell dimension. Here we use *small* cells of widths near to the characteristic swirl size in order to study size effects on the fluctuation amplitudes. Results are plotted in Fig. 4 where we look at the deviations from the power law fits of Eq. (3) versus the normalized cell widths $W/a\phi^{-1/3}$. The striking

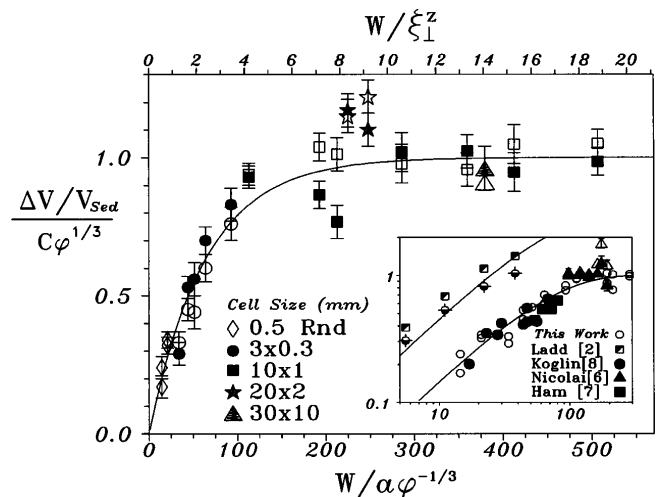


FIG. 4. Fluctuation amplitudes $\Delta V/V_{\text{sed}}$ (\parallel , closed symbols, and \perp , open symbols) divided by $(2.0, \parallel; 1.0, \perp) \times \phi^{1/3}$ versus the normalized cell width $W/a\phi^{-1/3}$. The cell size designations are width \times depth. Inset: Highlight of smallest cells, along with results from four previous studies.

feature of the main plot is the presence of an initial transition region in which $\Delta V_{\parallel,\perp}/V_{\text{sed}}$ has a strong cell size dependence, and above which the data are independent of the cell size. The inset highlights the transition region, and shows that the simple form,

$$\frac{\Delta V_{\parallel,\perp}}{V_{\text{sed}}} = C_{\parallel,\perp} \phi^{1/3} \left[1 - \exp\left(\frac{-W}{60a\phi^{-1/3}}\right) \right], \quad (4)$$

fits our data reasonably well. As shown in the inset, results from three previous experiments [6–8], conducted with particles 2 orders of magnitude larger than ours sedimenting in much more viscous liquids so as to keep the Reynolds number small ($\text{Re} \approx 10^{-3}$), collapse onto the same universal curve that describes our data. Results from a numerical simulation [2], though shifted roughly by a factor of 3, follow the same general trend. In summary, the shape of the universal curve illustrates how experiments with a limited range of cell sizes can lead to differing conclusions regarding the dependence of the fluctuation amplitudes upon cell size.

Regarding the dependence of the fluctuation amplitudes on cell geometry, we first note that all the cells (except the smallest, cylindrical cell) used in Fig. 4 had widths W larger than their thicknesses D . For the specific influence of the smaller dimension, we examine the results in cells in which W is much larger than the characteristic swirl size, $W \geq 5\xi_{\perp}^z$, and D varies from much smaller to much larger than ξ_{\perp}^z , $13 \leq D/a\phi^{-1/3} \leq 130$. These points are located in the saturation regime of Fig. 4 and illustrate, as found previously in Ref. [3], that to within error bars the results are independent of the cells' smallest dimension.

The dependencies found for the variance and the correlation lengths are interrelated by a simple heuristic argument. If the particle positions are uncorrelated (random) then the average number of particles in a region of size L is $N_L = L^3\phi/v_p$, where $v_p = (4/3)\pi a^3$ is the volume of one particle, and the fluctuations are $\Delta N_L = (N_L)^{1/2}$. The region is heavier or lighter than the average by the fluctuation in the number of particles. Its velocity fluctuation can then be related to its size by equating the buoyant mass force, $\Delta F_g = \Delta N_L v_p \Delta \rho g = \sqrt{L^3\phi v_p} \Delta \rho g$, to the viscous damping force $\Delta F_L = (6\pi\eta L)\Delta V$, yielding $\Delta V/V_0 = L^{1/2}\sqrt{\phi a^2/v_p}$. This suggests that the velocity difference increases with separation as in turbulent flows, that the variance depends upon the largest length scale of the system $L \sim W$, and diverges with the system size as $W^{1/2}$ [1,2]. This divergence will be contained only if the particles are correlated, not randomly distributed, above some cutoff length. The fact that we do not see a divergent velocity variance allows us to predict the correlation size ξ . Inverting $\Delta V/V_0 = L^{1/2}\sqrt{\phi a^2/v_p}$ with $L = \xi$ gives $\xi = (\Delta V/V_0)^2 v_p / \phi a^2$. Using the measured values of $\Delta V/V_{\text{sed}} = 2.0\phi^{1/3}$, and putting $V_0 = V_{\text{sed}}$ for our dilute samples, we find the correlation size as

$$\xi = (16\pi/3)a\phi^{-1/3} \approx 17a\phi^{-1/3}, \quad (5)$$

which is in close agreement with the measured correlation lengths represented by Eq. (2). Note that a direct consequence of the $\xi \sim \phi^{-1/3}$ scalings found in Eqs. (2) and (5) is that the average number of particles in each correlated region, $N_{\xi} = (2\xi_{\parallel})(\xi_{\perp}^2)\phi/v_p \approx 3000$, is independent of ϕ .

The large question which remains is how the hydrodynamic interactions from the sedimenting particles can induce the correlations which suppress the density fluctuations at length scales larger than ξ . There are calculations for the effects of hydrodynamic screening, but the predicted screening [5] length dependence of $l \sim \phi^{-1}$ is quite different than our finding of $\xi \sim \phi^{-1/3}$. We are not aware of any predictions for the spatial correlation functions $C_z(\mathbf{r})$. We note that the scaling of ξ with $a\phi^{-1/3}$ is not a trivial consequence of the dependence of the hydrodynamic interactions on distance ($1/r$). For a random distribution of particles there is no characteristic length. The scaling $\xi \sim \phi^{-1/3}$ is trivial only if the particles are correlated apart, i.e. fixed on a lattice, or if, as we have found, the correlated regions contain a fixed number of particles.

In conclusion, we have found a simple scaling of the amplitudes and spatial correlation functions of the velocity fluctuations that indicates that the settling dynamics at different values of ϕ are similar when scaled by the mean interparticle spacing ($a\phi^{-1/3}$). Fluctuation amplitudes were found to vary with cell size only for cells of dimensions less than the characteristic swirl size. No evidence for diverging fluctuations are found.

We thank Maarten Rutgers, Alex Levine, and Bill Russel for fruitful discussions.

*Present address: Department of Physics, University of Pennsylvania, Philadelphia, PA 19104.

†Also at Department of Physics, Princeton University, Princeton, NJ 08540.

- [1] R. E. Caflisch and J. H. C. Luke, *Phys. Fluids* **28**, 259 (1985).
- [2] A. J. C. Ladd, *Phys. Rev. Lett.* **76**, 1392 (1996).
- [3] H. Nicolai and E. Guazzelli, *Phys. Fluids* **7**, 3 (1995).
- [4] J.-Z. Xue, E. Herbolzheimer, M. A. Rutgers, W. B. Russel, and P. M. Chaikin, *Phys. Rev. Lett.* **69**, 1715 (1992).
- [5] D. L. Koch and E. S. G. Shaqfeh, *J. Fluid. Mech.* **224**, 275 (1991).
- [6] H. Nicolai, B. Herzhaft, E. J. Hinch, L. Oger, and E. Guazzelli, *Phys. Fluids* **7**, 12 (1995).
- [7] J. M. Ham and G. M. Homsy, *Int. J. Multiph. Flow* **14**, 533 (1988).
- [8] J. E. Koglin, Ph.D. thesis, Karlsruhe, Germany, 1971.
- [9] M. A. Rutgers, Ph.D. thesis, Princeton University, 1995.
- [10] R. J. Adrian, *Annu. Rev. Fluid Mech.* **23**, 261 (1991).